Published in final edited form as:
J Neurochem. 2008 February ; 104(4): 1006–1019. doi:10.1111/j.1471-4159.2007.05029.x.

Crustacean dopamine receptors: localization and G protein coupling in the stomatogastric ganglion

Merry C. Clark, **Reesha Khan**, and **Deborah J. Baro**
Program for Cell and Molecular Biology and Physiology, Department of Biology, Georgia State University, Atlanta, Georgia, USA

Abstract

Neuromodulators, such as dopamine (DA), control motor activity in many systems. To begin to understand how DA modulates motor behaviors, we study a well-defined model: the crustacean stomatogastric nervous system (STNS). The spiny lobster STNS receives both neuromodulatory and neurohormonal dopaminergic input, and extensive background information exists on the cellular and network effects of DA. However, there is a void of information concerning the mechanisms of DA signal transduction in this system. In this study, we show that Gs, Gi, and Gq are activated in response to DA in STNS membrane preparations from five crustacean species representing distant clades in the order Decapoda. Three evolutionarily conserved DA receptors mediate this response in spiny lobsters: $D_{1\alpha Pan}$, $D_{1\beta Pan}$ and $D_{1\alpha Pan}$. G protein coupling for these receptors can vary with the cell type. In the native membrane, the $D_{1\alpha Pan}$ receptor couples with Gs and Gq, the $D_{1\beta Pan}$ receptor couples with Gs, and the $D_{2\alpha Pan}$ receptor couples with Gi. All three receptors are localized exclusively to the synaptic neuropil and most likely generate global biochemical signals that alter ion channels in distant compartments, as well as local signals.

Keywords

central pattern generator; G protein-coupled receptor; identified neuron; invertebrate; neuromodulation; signal transduction

The neurotransmitter dopamine (DA) is associated with motor control in a variety of systems (Sidhu *et al.* 2003). In order to better understand how DA modulates motor behaviors, we study a well-established model system: the crustacean stomatogastric nervous system (STNS; Fig. 1) (Marder and Bucher 2006). The STNS is a peripheral nervous system whose sole function is to control the movements of the striated muscles surrounding the gut. The neurons in the STNS comprise multiple well-defined circuits. Each of these circuits is a central pattern generator (CPG) that drives a different set of muscles around the gut to produce a rhythmic, patterned motor activity associated with a specific function, such as chewing or swallowing.

Address correspondence and reprint requests to D.J. Baro, Biology Department, Georgia State University, P.O. Box 4010, Atlanta, GA 30303, USA. dbaro@gsu.edu.

Dopamine acts as both a neuromodulator and a neurohormone in the STNS (Kushner and Maynard 1977; Sullivan *et al.* 1977; Barker *et al.* 1979; Kushner and Barker 1983; Bucher *et al.* 2003). DA is found in descending modulatory input fibers that travel through the stomatogastric nerve (stn) to terminate in the neuropil of the stomatogastric ganglion (STG) (Fig. 1). The somata of these fibers originate in both the commissural ganglia (COG; Fig. 1) and the brain. Neurons in the STG do not themselves contain DA. Additionally, DA is secreted directly into the hemolymph by the pericardial organs, which are not shown in Fig. 1 (Sullivan *et al.* 1977; Fort *et al.* 2004). Importantly, the STG resides in an artery, and STG neurons are constantly bathed by hemolymph and therefore receive neurohormonal dopaminergic input.

DA's effects on the pyloric CPG have been particularly well characterized. The fourteen pyloric neurons are located exclusively within the STG (Fig. 1). Specific dopaminergic inputs to pyloric neurons have not been defined, but DA is known to reconfigure pyloric circuit output by altering component neuron intrinsic firing properties, synaptic strengths and axonal spike initiation (Selverston and Miller 1980; Anderson and Barker 1981; Eisen and Marder 1984; Marder and Eisen 1984; Flamm and Harris-Warrick 1986a, b; Harris-Warrick and Flamm 1987; Johnson and Harris-Warrick 1990; Johnson *et al.* 1995, 2005; Ayali and Harris-Warrick 1998, 1999; Bucher *et al.* 2003; Szucs *et al.* 2005). Many types of voltage-dependent ionic conductances are modified by bath applied DA, including a variety of K^+-, Ca^{2+}- and non-specific cation, or H-currents (Harris-Warrick *et al.* 1995a,b; Kloppenburg *et al.* 1999, 2000; Peck *et al.* 2001, 2006; Johnson *et al.* 2003; Gruhn *et al.* 2005). DA also modulates ionotropic receptors including a glutamategated chloride channel (Cleland and Selverston 1995, Cleland and Selverston 1997, Cleland and Selverston 1998). DA can modify multiple currents in a single cell type, and its effect on a given current is cell-specific; thus, DA evokes a unique response from each of the six pyloric cell types. The molecular mechanisms underlying these DA-induced cellular and circuit reconfigurations are poorly understood.

Dopaminergic responses are mediated by multiple, highly conserved DA receptors (DARs) that belong to the superfamily of G protein-coupled receptors (GPCRs). GPCRs often exist in multiprotein complexes, and their signaling pathways are constrained and shaped by proteins that co-localize in the receptor complex (Bockaert *et al.* 2003). GPCR signaling is context-dependent. Whereas the inherent properties of the GPCR are important, signaling pathways change according to the cellular milieu (Clark and Baro 2007). Moreover, GPCR signaling is not constant within a given cell type. Rather, GPCR performance can vary with its history of prior activation (Gainetdinov *et al.* 2004).

Dopamine receptors are broadly classified into two subfamilies on the basis of conserved structure and signaling mechanisms: D_1 and D_2 (Neve *et al.* 2004). Traditionally, DARs are thought to couple with trimeric G proteins: D_1 receptors activate $G\alpha_s$, whereas D_2 receptors couple with $G\alpha_{i/o}$ proteins. In addition to these two canonical cascades, DARs can couple with multiple G proteins (Sidhu and Niznik 2000), and signal through a variety of other means, including $G\beta\gamma$- (Clark and Baro 2007) and even G protein-independent-pathways (Beaulieu *et al.* 2005; Lefkowitz and Shenoy 2005; Zou *et al.* 2005). DARs can display agonist-independent activity (Hall and Strange 1997), and homo- and hetero-multimers can

form between DARs within a subfamily (Guo *et al.* 2003; Lee *et al.* 2003; Maggio *et al.* 2003).

There are three known DARs in arthropods. We have cloned the spiny lobster orthologs, $D_{1\alpha Pan}$, $D_{1\beta Pan}$, and $D_{2\alpha Pan}$, and characterized them in a heterologous expression system (Clark and Baro 2006, Clark and Baro 2007). We found that when stably expressed in human embryonic kidney (HEK) cells, $D_{1\alpha Pan}$ receptors coupled with Gs to increase cAMP, and $D_{1\beta Pan}$ receptors coupled with Gs and Gz to increase cAMP (Clark and Baro 2006). On the other hand, $D_{2\alpha Pan}$ receptors coupled with multiple members of the Gi/o family in HEK cells. Once activated, the Gα subunits of the trimeric Gi/o proteins acted to decrease cAMP, while the Gβγ subunits caused an increase in cAMP. Under the experimental conditions, the two effects summed. Thus, an increase or decrease in cAMP could be observed depending upon which cascade dominated the response, and the dominant cascade varied with the cell line (Clark and Baro 2007). The latter study emphasizes that DAR signaling is context-dependent, and dopaminergic transduction cascades must therefore be delineated in the native system. In this study, we define DAR-G protein couplings and localization in the STNS.

Materials and methods

Production of receptor-specific antagonists

Each of the three peptides shown below served as an antigen in the production of a rabbit, polyclonal, affinity-purified antibody that then functioned as the indicated receptor-specific antagonists (RSA). The peptides and antibodies were generated by the designated commercial establishments.

$D_{1\alpha}$ RSA antigen: CLDRYWAITDPFSYPSRM (Bethyl Laboratories Inc., Montgomery, TX, USA).

$D_{1\beta}$ RSA antigen: CDRYIHIKDPLRYGRWMTKRI (Bethyl Laboratories Inc.).

$D_{2\alpha}$ RSA antigen: CDRYIAVTQPIKYAQSKNNKR (Alpha Diagnostic International, San Antonio, TX, USA).

In addition to the antibodies that served as RSAs, an additional rabbit, polyclonal, affinity-purified antibody was generated against each receptor using the following extracellular antigens.

anti-D1α-AB.b: WRAVSDPHPVGACPFTEDL (Alpha Diagnostic).

anti-D1β-AB.b: VNDLLGYWPFGSQFCNIWIA (Alpha Diagnostic).

anti-D2α-AB.b: VNAISKKTQNPSLEPGC + CLAQTLPVLKVPNLKY (21st Century Biochemicals, Marlboro, MA, USA).

Membrane preparations

Membrane preparations for G protein assays on HEK cell lines were as previously described (Clark and Baro 2006, Clark and Baro 2007). For G protein assays on native tissue, an STNS was dissected from an animal and immediately frozen at) −70°C. STNS were homogenized on ice using a 2 mL Wheaton glass tissue grinder and ice-cold homogenizing buffer (120 mmol/L NaCl, 5 mmol/L KCl, 1.6 mmol/L KH_2PO_4, 1.2 mmol/L $MgSO_4$, 25 mmol/L $NaHCO_3$, 7.5 mmol/L dextrose, 2 mmol/L EGTA, 5 μg/mL leupeptin, 10 μg/mL aprotinin, 5 μg/mL pepstatin, 0.5 mg/mL Pefablock, 50 μL/mL Pefablock protector, 5 mmol/L iodoacetamide, and 1 mmol/L EDTA, pH 7.4). The homogenate was spun for 2 min at 0.4 *g*. The supernatant was recovered and centrifuged at 14 000 *g* for 30 min at 4°C. Pellets were resuspended in 20 mmol/L HEPES (pH 7.4) containing 0.5% 3-[(3-cholamidopropyl) dimethylammonio]-1-propanesulfonate (CHAPS), and 2 mmol/L EDTA, and shaken on ice for 1 h. Samples were then centrifuged for 1 min at 0.4 *g*, and supernatant was transferred to a fresh tube for storage at) −70°C. Protein concentrations were determined using a BCA Protein Assay Kit (Pierce, Rockford, IL, USA).

G protein activation assay

Agonist-induced activation of specific G proteins was determined as previously described (Clark and Baro 2006, Clark and Baro 2007). In this assay, binding of $GTP\gamma S^{35}$ to a given G protein is used as an index of G protein activation in the presence and absence of DA. This method employs commercially available antibodies against human G proteins (anti-Gs, anti-Gi and anti-Gq). This is valid because the antibodies were raised against the C-termini of human $G\alpha_s$, $G\alpha_q$, and $G\alpha_{i1/2}$, which are completely conserved with lobster $G\alpha_s$, $G\alpha_q$, and $G\alpha_i$, respectively (Clark and Baro 2006), and the antibodies specifically recognize their cognate lobster G proteins in immunoblot experiments (Fig. 2). In addition, a scan of the NCBI protein sequence database shows that $G\alpha_s$ and $G\alpha_q$ have also been sequenced from a penaeid shrimp (Dendrobranchiata, Fig. 3), and the C-termini are completely conserved. Literature and the insect genome database searches suggest that there are six Gα proteins in arthropods: $G\alpha_s$, $G\alpha_f$, $G\alpha_q$, Gαi, $G\alpha_o$, and $G\alpha_{12}$ (a.k.a. concertina).We did not examine receptor coupling with $G\alpha_f$, $G\alpha_o$, and $G\alpha_{12}$ in this work for lack of the appropriate sequence information and/or antibodies.

Immunoblots and immunocytochemistry

Antibodies were used in immunoblots and immunocytochemistry (ICC) protocols as previously described (Baro *et al.* 2000; Clark *et al.* 2004). Controls in which the antibodies were pre-absorbed with their cognate peptide antigens were performed for all antibodies in both types of experiments. In the case of the western blots and the ICC experiments using anti-$D_{2\alpha}$,-AB.b, all immunoreactivity was lost upon pre-absorption (not shown). In the case of ICC experiments using anti-$D_{1\alpha}$-AB.b or anti-$D_{1\beta}$ RSA, most immunoreactivity was lost upon pre-absorption, however, there was still some non-specific immunoreactivity homogeneously dispersed throughout the STG (not shown). In these cases, antibody specificity was confirmed with quantitative ICC experiments. Six independent experiments were performed for each antibody: three using the antibody and three using pre-absorbed antibody. For a given animal, five confocal stacks (10 μm) were obtained from the fine

neuropil where receptors appeared to reside (see Results). Receptor staining was quantified by counting all puncta in every 1 μm optical section in each confocal stack. Significant differences between experimental and pre-absorbed controls were determined with two-tailed, unpaired Student *t*-tests. As expected, the number of puncta in the synaptic neuropil was significantly increased by 5 ± 0.002-fold ($D_{1\alpha Pan}$, $p = 0.0014$) and 4.7 ± 0.008-fold ($D_{1\beta Pan}$, $p < 10^{-5}$), in the experimental compared to the pre-absorbed control.

In some ICC experiments, prior to fixation a neuron was filled with a lysine fixable, dextran-coupled Texas Red fluorophore that cannot pass through gap junctions (MW 10 000; Molecular Probes, Carlsbad, CA, USA). This was accomplished by pressure injecting a 1% solution of the fluorophore in 0.2 mol/L KCl using 20 ms pulses at 0.05 Hz and 28 psi for 10 min. The fluorophore was allowed to diffuse at 23 °C for > 2 h. The ganglion was then fixed and the standard ICC protocol performed.

semi-quantitative measurement of G protein abundance

The aforementioned G protein antibodies were used to quantify levels of G proteins in membrane preparations from the lobster nervous system relative to $D_{2\alpha Pan}$ receptor proteins. Two sets of experiments were performed. First, immunoblots containing lobster nervous system membrane protein extracts were probed with anti-D2α-AB.b and either anti-Gs, anti-Gi or anti-Gq (Fig. 2). The optical density (OD) for each signal was obtained, and the G protein signal was normalized by the $D_{2\alpha Pan}$ signal. These experiments were repeated three times with three different membrane protein extracts to obtain a relative measure of average G protein abundance for Gs (3.7 ± 1.1), Gi (0.5 ± 0.1) and Gq (2.1 ± 0.3). In order to compare these relative measures across G protein subtypes, a second set of experiments was performed to determine the efficiency of each G protein antibody. Dot blots containing 50 μg of each of the three antigenic G protein peptides were generated (http://www.abcam.com/technical) and subjected to the standard immunoblot protocol. For a given experiment (i.e., three dot blots: Gs, Gi, Gq), after removing the primary antibody, the dot blots were processed together and treated in an identical fashion for the remainder of the protocol. These experiments were repeated three times and the average OD of the immunogenic signal produced by each primary was found to be 414 ± 71, 381 ± 65 and 563 ± 119 for anti-Gs, anti-Gi, and anti-Gq, respectively. The data suggest that there were no statistically significant differences in antibody efficiencies (one-way ANOVA, $p = 0.49$). Nevertheless, the anti-Gq signal was 1.35 times more intense than Gs and 1.48 times more intense than Gi. To compensate for the differences in efficiencies, the average, relative G protein abundance determined in the first set of experiments was multiplied by 1.35 (Gs) or 1.48 (Gi). Data were analyzed with a one-way ANOVA.

Animals

Pacific spiny lobsters (*Panulirus interruptus*) were obtained from Don Tomlinson Commercial Fishing (San Diego, CA, USA). Lobsters were maintained at 16°C in constantly aerated and filtered seawater. Freshwater prawns (*Macrobrachium rosenbergii*) were obtained from the Kentucky State University Aquaculture Program (Frankfort, KY, USA). Animals were kept in filtered, aerated freshwater and killed within 24 h of arrival. Pink shrimp (*Penaeus duorarum*) were obtained from Gulf Specimen Marine Laboratories

Inc. (Panacea, FL, USA). Animals were kept in filtered, aerated seawater and killed within 48 h of arrival. Live American lobsters (*Homarus americanus*) and blue crabs (*Callinectes sapidus*) were obtained from the Dekalb Farmer's Market (Decatur, GA, USA) and kept on ice for up to 4 h from the time of purchase before killing. All animals were anesthetized by cooling on ice prior to experiments.

Statistical analyses and curve fitting

Student *t*-tests were performed with Excel software. Curve fitting and Kruskall–Wallis (ANOVA on ranks) tests were performed with Prism software. In all cases, statistical significance was determined as $p < 0.05$.

Results

DA activates Gs, Gi and Gq in STNS membranes in all species examined

DA-induced signal transduction cascades have never been defined in crustaceans. Although DARs can transduce signals through a variety of pathways, G protein cascades remain a major form of DAR-mediated signal transduction in all species examined. As a first step in characterizing DAR transduction cascades in the crustacean STNS, we examined DA-induced G protein activation in STNS membrane preparations from multiple crustacean species (Fig. 3). Recent studies on the phylogenetic relationships between Decapod crustaceans are summarized in the cladogram as shown in Fig. 3a (Richter and Scholtz 2001; Dixon *et al.* 2003). STNS circuits have been described for Dendrobranchiata (Tazaki and Tazaki 2000), Caridea (Meyrand and Moulins 1988) and Reptantia (Selverston and Moulins 1987; Harris-Warrick *et al.* 1992; Katz and Tazaki 1992). We examined five species spanning these three taxa. The data indicate that dopaminergic responses in the STNS are mediated by Gs, Gi, and Gq in all species examined (Fig. 3b), as is the case in the mammalian and *C. elegans* CNS. Although the mean DA-induced increase in Gs activity varied greatly with the species (e.g., compare the DA-induced fold change in Gs activity in lobster vs. freshwater prawn), there were no statistically significant differences in DA-induced G protein activity across species, as determined with one-way ANOVAs for Gs ($p > 0.078$), Gi ($p > 0.3$) and Gq ($p > 0.48$).

In some cases, the level of G protein activation within a given species varied according to the G protein. For example, Fig. 3(b) indicates that on average, DA increased Gs activity 4.6-fold, Gi activity 2.6-fold and Gq activity 2.2-fold in *Panulirus* membrane preparations. This could reflect differences in DAR and/or G protein abundances or efficacies. To determine if these changes correlated with the number of G proteins in the membrane preparation, we performed a semi-quantitative immunoblot analysis as described in Materials and methods, and found that Gs was approximately 2.4-fold more abundant than Gq ($p > 0.05$) and roughly 6.4-fold more abundant than Gi ($p < 0.03$), while Gq was about 4.0-fold more abundant than Gi ($p > 0.05$). These data suggest that the level of G protein activation did not strictly correlate with G protein abundance in the membrane preparation.

STG DARs are localized to the synaptic neuropil

Dopamine-induced activation of multiple G proteins is consistent with the fact that there are three known DARs in arthropods. In order to determine which DARs might contribute to the dopaminergic effects observed in Fig. 3(b), we ascertained receptor distributions in the spiny lobster STG. First, affinity-purified antibodies for each of the spiny lobster DARs were generated as described in Materials and methods. The immunoblots in Fig. 4 demonstrate that each of the antibodies recognized a protein larger than the predicted molecular weight, indicating putative post-translational processing of the receptor (glycosylation, phosphorylation, etc). The two bands recognized by the antibody against $D_{1\alpha Pan}$ most likely represent alternate splicing of receptor transcripts (Clark and Baro 2006, Clark and Baro 2007).

The antibodies were next used to determine receptor distributions in the native system. The STG is a highly structured ganglion containing roughly 30 neurons. STG anatomy has been well-characterized at the level of light and electron microscopy (King 1976a,b; Kilman and Marder 1996; Cabirol-Pol *et al.* 2002), and is diagramed in Fig. 5(a) and (b). The STG can be divided into three regions. The outer or peripheral layer contains the neuronal cell bodies. The central core, or coarse neuropil, contains large diameter neurites. The fine neuropil, which contains small diameter neurites, lies between the central coarse neuropil and the outer peripheral layer. STG synapses are exclusively confined to this region, so it is also known as the synaptic neuropil (King 1976b). As shown in Fig. 5(a), a monopolar STG neuron, whose soma lies in the peripheral layer, sends its primary process into the central coarse neuropil where it divides to produce several large diameter secondary and tertiary processes. These neurites then extend into the fine neuropil where they further divide and make synaptic contacts with other STG neurons, as well as the terminals of sensory and projection neurons. In sum, each of the three layers of the STG contains distinct neuronal subcellular compartments.

The well-defined STG architecture allows subcellular localization of neuronal proteins using confocal microscopy in conjunction with ICC experiments on STG wholemounts (Baro *et al.* 2000; Clark *et al.* 2004). Using this approach, we discovered that DARs were localized exclusively to neurolemma in the STG synaptic neuropil. Low magnification confocal stacks through the STG suggested that DARs were found predominantly in the fine neuropil (e.g., compare region of obvious immunostaining in Fig. 5c with horizontal section in Fig. 5b). Projections of high magnification confocal stacks from the fine neuropil showed that each of the three DARs displayed a punctate distribution throughout this region (Fig. 5d-f). STG neurons are entirely ensheathed by glial cells except at their synaptic terminals (King 1976b). We were interested in whether DARs localized to neurons and/or glia; therefore, in some experiments a single neuron was dye-filled prior to fixation and ICC. Examples of these experiments are shown in Fig. 5(g)–(i). The data illustrated that DARs were located in the terminals of ≤ 1 μm diameter processes, as well as in 3–10 μm bulbous structures emanating from fine neurites (arrowheads in Fig. 5g-i). Light and electron microscopic studies have previously shown that pre-synaptic compartments of spiny lobster STG neurons appear as 3–10 μm bulbous structures emanating from finer neurites, whereas post-synaptic compartments appear as ~1 μm finger-like projections extending from the pre-synaptic

compartments (King 1976b). DARs that were not located in the filled neurons (i.e., green immunoreactivity in Fig. 5g-i) exhibited the same staining pattern found for the filled neurons, suggesting that these DARs were most likely also localized to neurons, and not to glial cells. Finally, careful examination of 1 μm optical slices throughout an entire filled neuron and ganglia ($n \geq 3$ per antibody) indicated that DARs were never found in the plasma membrane surrounding the soma or large diameter neurites (not shown). Thus, the most parsimonious interpretation of our data is that DARs are in neuronal synaptic compartments located exclusively in the fine neuropil.

Generating receptor-specific antibody antagonists

The DA-induced increases in G protein activity observed in Fig. 3(b) represent the sum of all DAR-G protein couplings in the STNS. We next wanted to determine specific G protein couplings for each of the three lobster DARs. A RSA will subtract the contribution of an individual receptor from the summed DA-induced G protein activation, and thereby define receptor-G protein coupling. Accordingly, we set out to acquire a specific antagonist for each of the three DARs.

Since the pharmacology of invertebrate DARs is not well-characterized, and RSAs have not been identified, we created a specific antagonist for each receptor. The domains involved in receptor activation and G protein coupling have been fairly well defined and include the intracellular face of the third transmembrane domain and the adjacent intracellular loop 2 (*i2*) (Limbird 2004). The *i2* region is not highly conserved between the three DAR paralogs ($D_{1\alpha}$, $D_{1\beta}$, $D_{2\alpha}$) (Clark and Baro 2006, Clark and Baro 2007); thus, an anti-*i2* antibody could theoretically bind to its corresponding receptor and prevent it from activating G proteins.

To create RSAs, we generated three custom, affinity-purified antibodies against *i2*, one for each of the three *Panulirus* DARs: $D_{1\alpha}$ RSA, $D_{1\beta}$ RSA, and $D2_{\alpha}$ RSA. We tested each of the three potential RSAs for its ability to specifically block its cognate receptor in membrane preparations from previously described HEK cell lines, each stably expressing one of the three lobster DARs: HEK $D_{1\alpha Pan}$; HEK $D_{1\beta Pan}$; HEK $D_{2\alpha.1Pan}$ (Clark and Baro 2006, Clark and Baro 2007). Figs 6–8 illustrate that each antibody acts as an RSA.

The $D_{1\alpha Pan}$ receptor exclusively couples with Gs in HEK cells, but not members of the Gi/o, Gq, or G12 families of G proteins (Clark and Baro 2006). Figure 6a shows the effect of each RSA on $D_{1\alpha Pan}$-Gs coupling at the highest [RSA] tested (300 ng/mL). DA (10^{-5}mol/L) produced a significant, roughly 2-fold increase in Gs activity in these cells. The $D_{1\alpha}$ RSA completely blocked the DA-induced increase in Gs activity, while the $D_{1\beta}$ and the $D_{2\alpha}$ RSAs had no significant effect. Thus, only the $D_{1\alpha}$ RSA can uncouple the $D_{1\alpha Pan}$ receptor from Gs. Pre-absorption with its peptide antigen prevented $D_{1\alpha}$ RSA antagonism and the $D_{1\alpha}$ RSA had no significant effect on its own. Figure 6b illustrates the dose-dependencies of the 3 RSAs. Together these data indicate that only the $D_{1\alpha}$ RSA can uncouple the $D_{1\alpha Pan}$ receptor from Gs.

Next we tested the effect of the three RSAs on $D_{1\beta Pan}$ receptor-G protein coupling. When expressed in HEK cells, the $D_{1\beta Pan}$ receptor couples with Gs and Gz, but not members of

the Gq, or G12 families of G proteins, nor any member of the Gi/o family except Gz (Clark and Baro 2006). We performed G protein activation assays for Gs (Fig. 7a and b) and Gz (Fig. 7c and d) using HEK $D_{1\beta Pan}$ membranes with increasing concentrations of the RSAs. The $D_{1\beta}$ RSA blocked both of these couplings in a dose-dependent manner such that Gs and Gz activities in 10^{-5}mol/L DA plus 300 ng/mL $D_{1\beta}$ RSA were not significantly different than under baseline conditions. The $D_{1\beta}$ RSA could be inhibited by pre-absorption with its peptide antigen and had no effect on its own (Fig. 7a and c). As expected, the $D_{1\alpha}$ and $D_{2\alpha}$ RSAs had no significant effect on $D_{1\beta Pan}$ receptor-G protein couplings at any concentration tested. Together these data indicate that only the $D_{1\beta}$ RSA can prevent the $D_{1\beta Pan}$ receptor from coupling with G proteins.

The $D_{2\alpha Pan}$ receptor couples with multiple members of the Gi/o family, but not members of the Gs, Gq, or G12 families of G proteins (Clark and Baro 2007). Figure 8 demonstrates that the $D_{2\alpha}$ RSA disrupts all of these couplings in a dose-dependent manner, and reduces Gi/o activity to levels that are not significantly different from baseline. The $D_{2\alpha}$ RSA had no effect on its own and pre-absorption of the $D_{2\alpha}$ RSA with its peptide antigen prevented receptor antagonism (Fig. 8a, c and e). In contrast to the $D_{2\alpha}$ RSA, the $D_{1\alpha}$ and $D_{1\beta}$ RSAs had no significant effects on $D_{2\alpha Pan}$ coupling at any concentration tested. Thus, only the $D_{2\alpha Pan}$ RSA can uncouple the $D_{2\alpha Pan}$ receptor from G proteins. In summary, the data indicate that each of the three antibodies produces a significant dose-dependent decrease in receptor-G protein coupling for its cognate DAR, but not for any other DAR examined. Therefore, each antibody is a bona fide RSA.

$D_{1\alpha Pan}$ couples with Gs and Gq, $D_{1\beta Pan}$ couples with Gs and $D_{2\alpha Pan}$ couples with Gi in Panulirus STNS membranes

To determine DAR-G protein coupling in the lobster STNS, we performed G protein activation assays on lobster STNS membrane preparations in the presence and absence of DA and each of the RSAs. We reasoned that if an RSA could partially block some aspect of the DA response seen in Fig. 3(b), it would suggest that the corresponding receptor signals through the G protein whose activity had been reduced. These experiments are shown in Fig. 9. For a given experiment, the membrane preparations were tested with no DA and no RSA (baseline conditions, right panels in Fig. 9a–c) and with 10^{-5}mol/L DA and increasing concentrations of the indicated RSA (left panels in Fig. 9a–c). For each experiment all the data were normalized by G protein activity in the presence of 10^{-5}mol/L DA without RSA. Multiple experiments were averaged and the data are plotted as the percent of the response in 10^{-5}mol/L DAwithout RSA.

Figure 9a illustrates that DA increased Gs activity by 3.1 ± 0.08-fold ($p < 10^{-4}$, $n = 4$), Gq activity by 1.9 ± 0.06-fold ($p < 10^{-4}$, $n = 4$) and Gi activity by 3.2 ± 0.05-fold ($p < 10^{-5}$, $n = 4$). The $D_{1\alpha}$ RSA dose-dependently reduced the DA-induced increase in Gs and Gq, but not Gi activities. The DA-induced increase in Gs activity was significantly reduced by 300 ng/mL $D_{1\alpha}$ RSA ($p < 0.005$ for 0 vs. 300 ng/mL RSA) such that it was not significantly different from baseline ($p > 0.17$ for 300 ng/mL RSA vs. baseline). Similarly, the DA-induced increase in Gq activity was significantly reduced by 300 ng/mL $D_{1\alpha}$ RSA ($p < 0.002$) such that it was not significantly different from baseline ($p > 0.35$). On the other

hand, 300 ng/mL $D_{1\alpha}$ RSA had no significant effect on the DA-induced increase in Gi activity ($p > 0.7$). In sum, the data indicate that the $D_{1\alpha Pan}$ receptor couples with both Gs and Gq.

Figure 9b shows that the $D_{1\beta Pan}$ receptor couples solely with Gs in the spiny lobster STNS. Gs activity was significantly reduced in a dose-dependent fashion by the $D_{1\beta}$ RSA ($p < 10^{-4}$ for 0 vs. 300 ng/mL $D_{1\beta}$ RSA, $n = 3$). The $D_{1\beta}$ RSA reduced Gs activity to levels that were not significantly different than baseline ($p > 0.08$). On the other hand, there were no statistically significant changes in Gq ($p > 0.2$) or Gi ($p > 0.4$) activities in response to increasing concentrations of the RSA. Further, although it appears that Gi activity increases with increasing [D1β RSA], perhaps suggesting an interaction between Gs and Gi (e.g., competition for Gβγ subunits), a linear regression did not reveal a statistically significant correlation between the rise in Gi and the reduction in Gs activities with increasing [RSA].

Figure 9c illustrates that the lobster $D_{2\alpha Pan}$ receptor couples with Gi alone. At 200 ng/mL the $D_{2\alpha}$ RSA significantly reduced the DA-induced increase in Gi activity ($p < 0.02$, $n = 3$). Furthermore, at concentrations of 10 ng/mL or higher, the $D_{2\alpha}$ RSA reduced Gi activity to levels that were not significantly different than baseline ($p > 0.88$). On the other hand, the D2α RSA had no significant effect on DA-induced increases in Gs ($p > 0.9$) or Gq ($p > 0.68$) activities. In summary, the data suggest that $D_{1\alpha Pan}$ couples with Gs and Gq, $D_{1\beta Pan}$ couples with Gs and $D_{2\alpha Pan}$ couples with Gi in STNS membrane preparations.

Discussion

The crustacean STNS is an important model system for understanding the involvement of neuromodulators in motor control. It was previously shown that DA can alter CPG output by modulating multiple ionic conductances in component neurons in a cell-specific manner. DA altered the biophysical properties of ion channels throughout neurons, including channels in the soma and the neuropil. In this study, we begin to define the molecular mechanisms underlying these changes. We found that DA activates Gs, Gi and Gq in the STNS of all five crustacean species examined. Further, we demonstrated that the three known DARs were all expressed in the spiny lobster STG and were exclusively localized to the synaptic neuropil where the $D_{1\alpha Pan}$ receptor coupled with Gs and Gq, the $D_{1\beta Pan}$ receptor coupled with Gs and the $D_{2\alpha Pan}$ receptor coupled with Gi. The expression of multiple receptors with distinct G protein couplings in the STNS can help to explain the previously documented, cell-specific modulation of ionic conductances by DA.

In other systems, DARs are known to alter local target protein activity through multiple G protein-dependent and -independent mechanisms. Our data suggest that STNS DARs can also alter cell function locally through G protein transduction cascades. Unfortunately, our data do not predict how a given receptor will alter second messengers, but the literature suggests that STNS DARs will most likely modulate [cAMP] and [Ca^{2+}]. Regardless of the details, both Gα and Gβγ subunits will indirectly modulate local second messenger levels, and this in turn will alter kinase and phosphatase activities, which will modify the phosphorylation states of ion channels and thereby change neuronal excitability and circuit output. Independent of second messengers, the Gβγ subunits can also directly modulate ion

channels (Dascal 2001). In addition, Gβγ subunits are known to directly regulate the synaptic release machinery (Blackmer *et al.* 2005; Gerachshenko *et al.* 2005), which could partially account for DA-induced alterations in synaptic strengths within the circuit (Johnson and Harris-Warrick 1990).

STNS DARs may also generate more global signals. On the one hand, we have shown that DA-Rs are not in the plasma membrane surrounding pyloric somata or primary neurites. Indeed, DARs are at least hundreds of microns away from the primary neurite and are found exclusively in the neurolemma encompassing fine neurites and/or terminals in the synaptic neuropil (Fig. 5). On the other hand, two electrode voltage clamp studies suggest that DA alters somatic ion channels within seconds of application (Hartline *et al.* 1993; Kloppenburg *et al.* 1999). Together these data suggest that pyloric DARs might transduce constant bath applied DA into a global signal. Second messengers have the potential for rapid diffusion and could therefore propagate a global signal. One possibility is that at least some STNS DA-Rs produce global changes in cAMP since (i) previous imaging studies on STG neurons revealed that neuromodulator-induced increases in $[cAMP]_i$ were initially generated in the fine neurites and diffused to the soma with time (Hempel *et al.* 1996), (ii) STNS DA-Rs activate G protein cascades that modulate $[cAMP]_i$ (Clark and Baro 2006, Clark and Baro 2007), and (iii) experimental and computational studies on a variety of cell types have shown that GPCRs that couple with Gs can generate small and sustained global changes in $[cAMP]_i$ (Rich *et al.* 2001; Dyachok *et al.* 2006; Nikolaev *et al.* 2006; Rochais *et al.* 2006; Gervasi *et al.* 2007). Alternatively, DA-Rs may produce global changes in Ca^{2+}. Mammalian and arthropod D_1 (Reale *et al.* 1997) and D_2 receptors, including $D_{2\alpha Pan}$ (Tsu and Wong 1996; Clark and Baro 2007), are known to activate phospholipase-C-β via Gβγ subunits, and in some cases increase $[Ca^{2+}]_i$ (Nishi *et al.* 1997; Hernandez-Lopez *et al.* 2000). In addition, $D_{1\alpha Pan}$ receptors couple with Gq, which is traditionally thought to release Ca^{2+} stores. It might also be argued that second messenger effectors (i.e., proteins) rather than the second messengers themselves diffuse to the soma. Given the size difference, protein diffusion should be a much slower process. Moreover, it has been shown that in *Aplysia* neurons protein kinase A (PKA) is distinct in the soma (PKA I) and terminals (PKA II), and PKA I is responsible for activating nuclear cAMP response element-binding proteins in response to neuromodulators acting at distant terminals (Liu *et al.* 2004).

Our work reinforces the idea that receptor-G protein interactions are highly preserved throughout evolution. Spiny lobster DARs are not only highly conserved at the amino acid level, but they show the same couplings in native and heterologous systems as is observed with receptors from other species (Fig. 3, Clark and Baro 2006, Clark and Baro 2007). Interestingly, DA seemed to activate Gs to a lesser extent in *M. rosenbergii* than in other species (Fig. 3b). This could reflect a difference in DAR and/or G protein distribution patterns across species, but without sequence data we cannot rule out technical reasons for the variation. For example, the anti-Gs antibody used in the G protein assay may not recognize the *M. rosenbergii* Gs protein as well as the Gs protein in other species.

Finally, the data demonstrate that lobster DAR signaling is context-dependent. G protein couplings in the native system are different from those in HEK cell lines. The $D_{1\alpha Pan}$ receptor only couples with Gs in HEK cells (Clark and Baro 2006), but Gs and Gq in the

lobster STNS. $D_{1\beta Pan}$ couples with Gs and Gi/o protein families in HEK cells, but only Gs in the STNS. Differential coupling according to cell type has been reported for DARs from a variety of species and cell types (Sidhu and Niznik 2000). Together, these data suggest that a given DAR can interact with a limited repertoire of G proteins, and that the cellular environment further restricts the range of interactions and helps to define the specific DAR-G protein couplings that occur in a given cell type.

Acknowledgments

We thank Jin Kim and Jill Nakatani for excellent technical assistance. Additionally, we thank the Kentucky State University Aquaculture Program for the kind gift of *Macrobrachium rosenbergii*. We are indebted to Dr Jeremy M. Sullivan for sharing his insight on Decapod phylogeny and his excellent suggestions for Fig. 3(a). We also thank Dr Jens Herberholz for statistical advice. This work was supported, in part, by NIH NS38770. MCC is a fellow of the GSU Molecular Basis of Disease Program.

References

Anderson WW, Barker DL. Synaptic mechanisms that generate network oscillations in the absence of discrete postsynaptic potentials. J Exp Zool. 1981; 216:187–191. [PubMed: 7288387]

Ayali A, Harris-Warrick RM. Interaction of dopamine and cardiac sac modulatory inputs on the pyloric network in the lobster stomatogastric ganglion. Brain Res. 1998; 794:155–161. [PubMed: 9630592]

Ayali A, Harris-Warrick RM. Monoamine control of the pacemaker kernel and cycle frequency in the lobster pyloric network. J Neurosci. 1999; 19:6712–6722. [PubMed: 10415000]

Barker DL, Kushner PD, Hooper NK. Synthesis of dopamine and octopamine in the crustacean stomatogastric nervous system. Brain Res. 1979; 161:99–113. [PubMed: 365295]

Baro DJ, Ayali A, French L, Scholz NL, Labenia J, Lanning CC, Graubard K, Harris-Warrick RM. Molecular underpinnings of motor pattern generation: differential targeting of shal and shaker in the pyloric motor system. J Neurosci. 2000; 20:6619–6630. [PubMed: 10964967]

Beaulieu JM, Sotnikova TD, Marion S, Lefkowitz RJ, Gainetdinov RR, Caron MG. An Akt/beta-arrestin 2/Pp2a signaling complex mediates dopaminergic neurotransmission and behavior. Cell. 2005; 122:261–273. [PubMed: 16051150]

Blackmer T, Larsen EC, Bartleson C, Kowalchyk JA, Yoon EJ, Preininger AM, Alford S, Hamm HE, Martin TF. G Protein betagamma directly regulates snare protein fusion machinery for secretory granule exocytosis. Nat Neurosci. 2005; 8:421–425. [PubMed: 15778713]

Bockaert J, Marin P, Dumuis A, Fagni L. The 'Magic Tail' of G protein-coupled receptors: an anchorage for functional protein networks. FEBS Lett. 2003; 546:65–72. [PubMed: 12829238]

Bucher D, Thirumalai V, Marder E. Axonal dopamine receptors activate peripheral spike initiation in a stomatogastric motor neuron. J Neurosci. 2003; 23:6866–6875. [PubMed: 12890781]

Cabirol-Pol MJ, Combes D, Fenelon VS, Simmers J, Meyrand P. Rare and spatially segregated release sites mediate a synaptic interaction between two identified network neurons. J Neurobiol. 2002; 50:150–163. [PubMed: 11793361]

Clark MC, Baro DJ. Molecular cloning and characterization of crustacean type-one dopamine receptors: D1alphapan and D1betapan. Comp Biochem Physiol B Biochem Mol Biol. 2006; 143:294–301. [PubMed: 16426885]

Clark MC, Baro DJ. Arthropod D2 receptors positively couple with cAMP through the Gi/O protein family. Comp Biochem Physiol B Biochem Mol Biol. 2007; 146:9–19. [PubMed: 17134931]

Clark MC, Dever TE, Dever JJ, Xu P, Rehder V, Sosa MA, Baro DJ. Arthropod 5-Ht2 receptors: a neurohormonal receptor in decapod crustaceans that displays agonist independent activity resulting from an evolutionary alteration to the dry motif. J Neurosci. 2004; 24:3421–3435. [PubMed: 15056722]

Cleland TA, Selverston AI. Glutamate-gated inhibitory currents of central pattern generator neurons in the lobster stomatogastric ganglion. J Neurosci. 1995; 15:6631–6639. [PubMed: 7472424]

Cleland TA, Selverston AI. Dopaminergic modulation of inhibitory glutamate receptors in the lobster stomatogastric ganglion. J Neurophysiol. 1997; 78:3450–3452. [PubMed: 9405559]

Cleland TA, Selverston AI. Inhibitory glutamate receptor channels in cultured lobster stomatogastric neurons. J Neurophysiol. 1998; 79:3189–3196. [PubMed: 9636118]

Dascal N. Ion-channel regulation by G proteins. Trends Endocrinol Metab. 2001; 12:391–398. [PubMed: 11595540]

Dixon CJ, Ahyong ST, Schram FR. A new hypothesis of decapod phylogeny. Crustaceana. 2003; 76:935–975.

Dyachok O, Isakov Y, Sagetorp J, Tengholm A. Oscillations of cyclic AMP in hormone-stimulated insulin-secreting beta-cells. Nature. 2006; 439:349–352. [PubMed: 16421574]

Eisen JS, Marder E. A mechanism for production of phase shifts in a pattern generator. J Neurophysiol. 1984; 51:1375–1393. [PubMed: 6145759]

Flamm RE, Harris-Warrick RM. Aminergic modulation in lobster stomatogastric ganglion. Ii. target neurons of dopamine, octopamine, and serotonin within the pyloric circuit. J Neurophysiol. 1986a; 55:866–881. [PubMed: 3086514]

Flamm RE, Harris-Warrick RM. Aminergic modulation in lobster stomatogastric ganglion. I. Effects on motor pattern and activity of neurons within the pyloric circuit. J Neurophysiol. 1986b; 55:847–865. [PubMed: 3086513]

Fort TJ, Brezina V, Miller MW. Modulation of an integrated central pattern generator-effector system: dopaminergic regulation of cardiac activity in the blue crab *Callinectes sapidus*. J Neurophysiol. 2004; 92:3455–3470. [PubMed: 15295014]

Gainetdinov RR, Premont RT, Bohn LM, Lefkowitz RJ, Caron MG. Desensitization of G protein-coupled receptors and neuronal functions. Annu Rev Neurosci. 2004; 27:107–144. [PubMed: 15217328]

Gerachshenko T, Blackmer T, Yoon EJ, Bartleson C, Hamm HE, Alford S. Gbetagamma acts at the C-terminus of Snap-25 to mediate presynaptic inhibition. Nat Neurosci. 2005; 8:597–605. [PubMed: 15834421]

Gervasi N, Hepp R, Tricoire L, Zhang J, Lambolez B, Paupardin-Tritsch D, Vincent P. Dynamics of protein kinase a signaling at the membrane, in the cytosol, and in the nucleus of neurons in mouse brain slices. J Neurosci. 2007; 27:2744–2750. [PubMed: 17360896]

Gruhn M, Guckenheimer J, Land B, Harris-Warrick RM. Dopamine modulation of two delayed rectifier potassium currents in a small neural network. J Neurophysiol. 2005; 94:2888–2900. [PubMed: 16014791]

Guo W, Shi L, Javitch JA. The fourth transmembrane segment forms the interface of the dopamine D2 receptor homodimer. J Biol Chem. 2003; 278:4385–4388. [PubMed: 12496294]

Hall DA, Strange PG. Evidence that antipsychotic drugs are inverse agonists at D2 dopamine receptors. Br J Pharmacol. 1997; 121:731–736. [PubMed: 9208141]

Harris-Warrick RM, Flamm RE. Multiple mechanisms of bursting in a conditional bursting neuron. J Neurosci. 1987; 7:2113–2128. [PubMed: 3112322]

Harris-Warrick, RM.; Marder, E.; Selverston, AI.; Moulins, M., editors. Dynamic Biological Networks: The Stomatogastric Nervous System. MIT Press; Cambridge: 1992.

Harris-Warrick RM, Coniglio LM, Barazangi N, Guckenheimer J, Gueron S. Dopamine modulation of transient potassium current evokes phase shifts in a central pattern generator network. J Neurosci. 1995a; 15:342–358. [PubMed: 7823140]

Harris-Warrick RM, Coniglio LM, Levini RM, Gueron S, Guckenheimer J. Dopamine modulation of two subthreshold currents produces phase shifts in activity of an identified motoneuron. J Neurophysiol. 1995b; 74:1404–1420. [PubMed: 8989381]

Hartline DK, Gassie DV, Jones BR. Effects of soma isolation on outward currents measured under voltage clamp in spiny lobster stomatogastric motor neurons. J Neurophysiol. 1993; 69:2056–2071. [PubMed: 7688800]

Hempel CM, Vincent P, Adams SR, Tsien RY, Selverston AI. Spatio-temporal dynamics of cyclic AMP signals in an intact neural circuitm. Nature. 1996; 384:166–169. [PubMed: 8906791]

Hernandez-Lopez S, Tkatch T, Perez-Garci E, Galarraga E, Bargas J, Hamm H, Surmeier DJ. D2 dopamine receptors in striatal medium spiny neurons reduce L-type Ca^{2+} currents and excitability

via a novel Plc[Beta]1-Ip3-calcineurin-signaling cascade. J Neurosci. 2000; 20:8987–8995. [PubMed: 11124974]

Johnson BR, Harris-Warrick RM. Aminergic modulation of graded synaptic transmission in the lobster stomatogastric ganglion. J Neurosci. 1990; 10:2066–2076. [PubMed: 2165519]

Johnson BR, Peck JH, Harris-Warrick RM. Distributed amine modulation of graded chemical transmission in the pyloric network of the lobster stomatogastric ganglion. J Neurophysiol. 1995; 74:437–452. [PubMed: 7472345]

Johnson BR, Kloppenburg P, Harris-Warrick RM. Dopamine modulation of calcium currents in pyloric neurons of the lobster stomatogastric ganglion. J Neurophysiol. 2003; 90:631–643. [PubMed: 12904487]

Johnson BR, Schneider LR, Nadim F, Harris-Warrick RM. Dopamine modulation of phasing of activity in a rhythmic motor network: contribution of synaptic and intrinsic modulatory actions. J Neurophysiol. 2005; 94:3101–3111. [PubMed: 16014790]

Katz, PS.; Tazaki, K. Comparative and evolutionary aspects of the crustacean stomatogastric system. In: Harris-Warrick, RM.; Marder, E.; Selverston, AI.; Moulins, M., editors. Dynamic Biological Networks: The Stomoatogatric Nervous System. MIT Press; Cambridge: 1992. p. 221-262.

Kilman VL, Marder E. Ultrastructure of the stomatogastric ganglion neuropil of the crab, *Cancer borealis*. J Comp Neurol. 1996; 374:362–375. [PubMed: 8906505]

King DG. organization of crustacean neuropil. Ii. Distribution of synaptic contacts on identified motor neurons in lobster stomatogastric ganglion. J Neurocytol. 1976a; 5:239–266. [PubMed: 178837]

King DG. Organization of crustacean neuropil. I. Patterns of synaptic connections in lobster stomatogastric ganglion. J Neurocytol. 1976b; 5:207–237. [PubMed: 1271087]

Kloppenburg P, Levini RM, Harris-Warrick RM. Dopamine modulates two potassium currents and inhibits the intrinsic firing properties of an identified motor neuron in a central pattern generator network. J Neurophysiol. 1999; 81:29–38. [PubMed: 9914264]

Kloppenburg P, Zipfel WR, Webb WW, Harris-Warrick RM. Highly localized Ca(2+) accumulation revealed by multiphoton microscopy in an identified motoneuron and its modulation by dopamine. J Neurosci. 2000; 20:2523–2533. [PubMed: 10729332]

Kushner PD, Barker DL. A neurochemical description of the dopaminergic innervation of the stomatogastric ganglion of the spiny lobster. J Neurobiol. 1983; 14:17–28. [PubMed: 6402561]

Kushner PD, Maynard EA. Localization of monoamine fluorescence in the stomatogastric nervous system of lobsters. Brain Res. 1977; 129:13–28. [PubMed: 871924]

Lee SP, O'Dowd BF, Rajaram RD, Nguyen T, George SR. D2 dopamine receptor homodimerization is mediated by multiple sites of interaction, including an intermolecular interaction involving transmembrane domain 4. Biochemistry. 2003; 42:11023–11031. [PubMed: 12974638]

Lefkowitz RJ, Shenoy SK. Transduction of receptor signals by beta-arrestins. Science. 2005; 308:512–517. [PubMed: 15845844]

Limbird LE. The receptor concept: A continuing evolution. Mol Interv. 2004; 4:326–336. [PubMed: 15616162]

Liu J, Hu JY, Schacher S, Schwartz JH. The two regulatory subunits of aplysia cAMP-dependent protein kinase mediate distinct functions in producing synaptic plasticity. J Neurosci. 2004; 24:2465–2474. [PubMed: 15014122]

Maggio R, Scarselli M, Novi F, Millan MJ, Corsini GU. Potent activation of dopamine D3/D2 heterodimers by the antiparkinsonian agents, S32504, pramipexole and ropinirole. J Neurochem. 2003; 87:631–641. [PubMed: 14535946]

Marder E, Bucher D. Understanding circuit dynamics using the stomatogastric nervous system of lobsters and crabs. Annu Rev Physiol. 2006; 69:291–316. [PubMed: 17009928]

Marder E, Eisen JS. Electrically coupled pacemaker neurons respond differently to same physiological inputs and neurotransmitters. J Neurophysiol. 1984; 51:1362–1374. [PubMed: 6145758]

Meyrand P, Moulins M. Phylogenetic plasticity of crustacean stomatogastric circuits. I. pyloric opatterns and pyloric circuit of the shrimp *Palaemon serratus*. J Exp Biol. 1988; 138:107–132.

Neve KA, Seamans JK, Trantham-Davidson H. Dopamine receptor signaling. J Recept Signal Transduct Res. 2004; 24:165–205. [PubMed: 15521361]

Nikolaev VO, Bunemann M, Schmitteckert E, Lohse MJ, Engelhardt S. Cyclic AMP imaging in adult cardiac myocytes reveals far-reaching beta1-adrenergic but locally confined beta2-adrenergic receptor-mediated signaling. Circ Res. 2006; 99:1084–1091. [PubMed: 17038640]

Nishi A, Snyder GL, Greengard P. Bidirectional regulation of Darpp-32 phosphorylation by dopamine. J Neurosci. 1997; 17:8147–8155. [PubMed: 9334390]

Peck JH, Nakanishi ST, Yaple R, Harris-Warrick RM. Amine modulation of the transient potassium current in identified cells of the lobster stomatogastric ganglion. J Neurophysiol. 2001; 86:2957–2965. [PubMed: 11731552]

Peck JH, Gaier E, Stevens E, Repicky S, Harris-Warrick RM. Amine modulation of Ih in a small neural network. J Neurophysiol. 2006; 96:2931–2940. [PubMed: 16943317]

Reale V, Hannan F, Hall LM, Evans PD. Agonist-specific coupling of a cloned *Drosophila melanogaster* D1-like dopamine receptor to multiple second messenger pathways by synthetic agonists. J Neurosci. 1997; 17:6545–6553. [PubMed: 9254667]

Rich TC, Fagan KA, Tse TE, Schaack J, Cooper DM, Karpen JW. A uniform extracellular stimulus triggers distinct cAMP signals in different compartments of a simple cell. Proc Natl Acad Sci USA. 2001; 98:13049–13054. [PubMed: 11606735]

Richter S, Scholtz G. Phylogenetic Analyses of the *Malacostraca* (Crustacea). J Zool Systemat Res. 2001; 39:1–23.

Rochais F, Abi-Gerges A, Horner K, Lefebvre F, Cooper DM, Conti M, Fischmeister R, Vandecasteele G. A specific pattern of phosphodiesterases controls the cAMP signals generated by different Gs-coupled receptors in adult rat ventricular myocytes. Circ Res. 2006; 98:1081–1088. [PubMed: 16556871]

Selverston AI, Miller JP. Mechanisms underlying pattern generation in lobster stomatogastric ganglion as determined by selective inactivation of identified neurons. I. Pyloric system. J Neurophysiol. 1980; 44:1102–1121. [PubMed: 6256508]

Selverston, AI.; Moulins, M., editors. The Crustacean Stomatogastric System. Springer; Berlin: 1987.

Sidhu A, Niznik HB. Coupling of dopamine receptor subtypes to multiple and diverse G proteins. Int J Dev Neurosci. 2000; 18:669–677. [PubMed: 10978845]

Sidhu, A.; Laruelle, M.; Vernier, P., editors. Dopamine Receptors and Transporters: Function, Imaging and Clinical Implication. 2nd. Marcel Dekker, Inc; New York: 2003.

Sullivan RE, Friend BJ, Barker DL. Structure and function of spiny lobster ligamental nerve plexuses: evidence for synthesis, storage, and secretion of biogenic amines. J Neurobiol. 1977; 8:581–605. [PubMed: 340611]

Szucs A, Abarbanel HD, Rabinovich MI, Selverston AI. Dopamine modulation of spike dynamics in bursting neurons. Eur J Neurosci. 2005; 21:763–772. [PubMed: 15733094]

Tazaki K, Tazaki Y. Multiple motor patterns in the stomatogastric ganglion of the shrimp *Penaeus japonicus*. J Comp Physiol [A]. 2000; 186:105–118.

Tsu RC, Wong YH. Gi-mediated stimulation of type Ii adenylyl cyclase is augmented by Gq-coupled receptor activation and phorbol ester treatment. J Neurosci. 1996; 16:1317–1323. [PubMed: 8778283]

Zou S, Li L, Pei L, Vukusic B, Van Tol HH, Lee FJ, Wan Q, Liu F. Protein-protein coupling/uncoupling enables dopamine D2 receptor regulation of AMPA receptor-mediated excitotoxicity. J Neurosci. 2005; 25:4385–4395. [PubMed: 15858065]

Abbreviation used

DA	dopamine
DARs	DA receptors
GPCRs	G protein-coupled receptors
HEK	human embryonic kidney

ICC	immunoblots and immunocytochemistry
PKA	protein kinase A
RSA	receptor-specific antagonists
STG	stomatogastric ganglion
STNS	stomatogastric nervous system

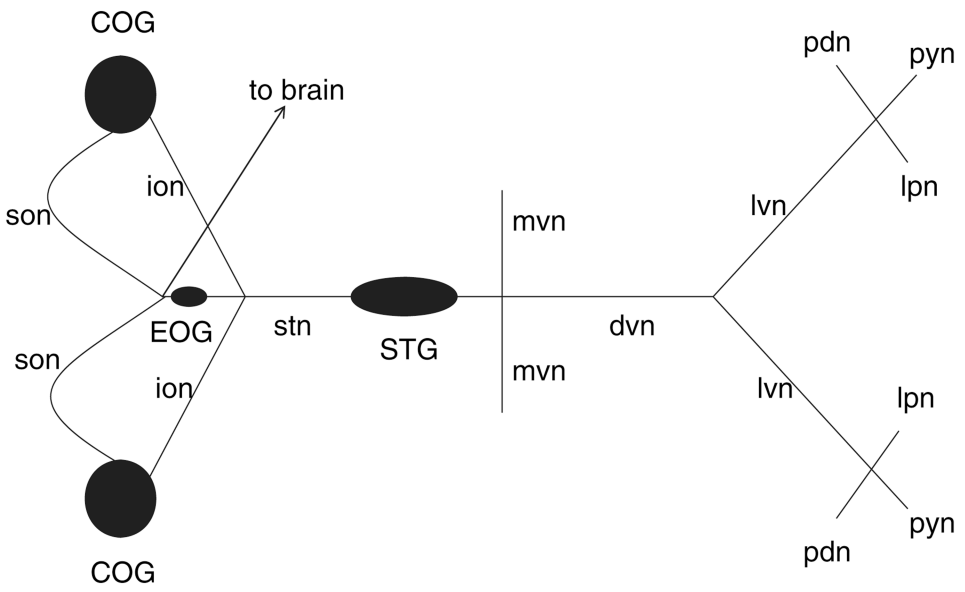

Fig. 1.

Diagram of the STNS. Ganglia are represented as *filled ovals* and *circles*. Ganglia contain the somatodendritic compartments of neurons. Neurons in one ganglion project their axons to another ganglion or to muscles via identified nerves, which are represented as *lines*. Monopolar neurons in the STG send their axons down the dvn to terminate on muscle fibers, or up the stn to terminate in the neuropil of higher ganglia (i.e., commissural ganglia, *COG*). DA containing neurons are located in the *COG* and brain, and send axons down the *stn* to terminate in the STG. *EOG*, esophageal ganglion; *ion*, inferior esophageal nerve; *son*, superior esophageal nerve; *stn*, stomatogastric nerve; *dvn*, dorsal ventricular nerve; *mvn*, medial ventricular nerve; *lvn*, lateral ventricular nerve; *lpn*, lateral pyloric nerve; *pyn*, pyloric nerve; *pdn*, pyloric dilator nerve.

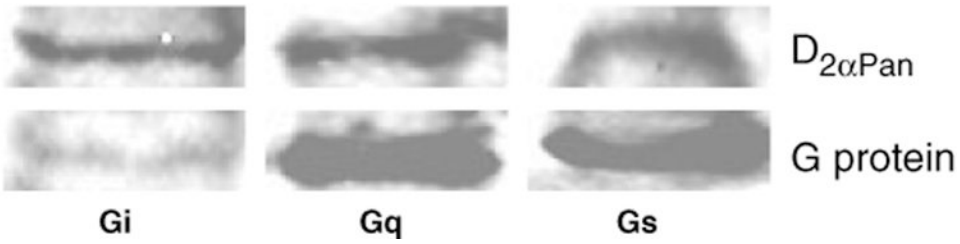

Fig. 2.

Gs, Gi and Gq are differentially expressed in the lobster. Western blots containing protein extracts from the lobster nervous system were probed with antibodies against $D_{2\alpha Pan}$ and Gαi, Gαq, or Gαs. The human G protein antibodies recognized lobster G proteins of predicted molecular weights (Gαi ~ 36 kDa, Gαq ~ 36 kDa, Gαs ~ 37 kDa).

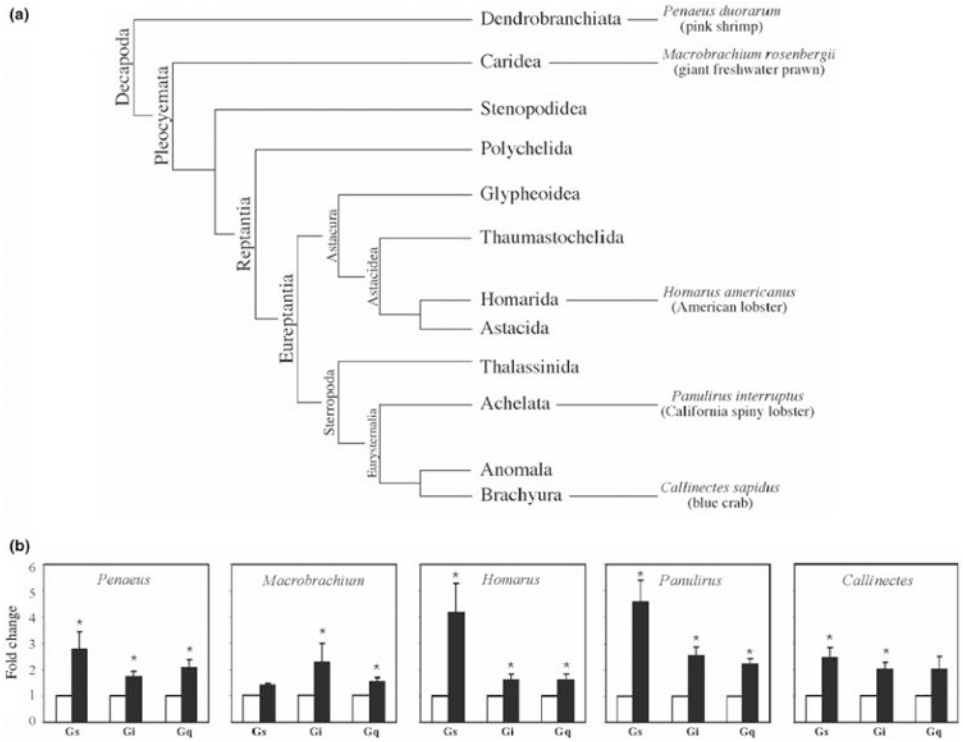

Fig. 3.

Dopaminergic responses in the STNS are mediated by Gs, Gi, and Gq in all species of Decapod crustaceans examined. (a) Phylogenetic classification scheme for Decapod crustaceans modified from (Dixon *et al.* 2003). Branches are not drawn to scale. (b) DA activates Gs, Gi and Gq in all species examined. G protein activity in the absence (open bar) versus the presence (filled bar) of 10^{-5}mol/L DA was measured for Gs, Gi, and Gq in STNS membrane preparations from multiple species, as indicated. For each species, the total number of animals used for all experiments, and the total number of independent experiments are: 25 *Penaeus*, $n = 5$ experiments; 13 *Machrobrachium*, $n = 3$; 30 *Panulirus*, $n = 17$; 10 *Homarus*, $n = 7$; 20 Callinectes, $n = 5$. The activities of all three G proteins were measured in each experiment. Data are represented as the mean ± SEM. Statistically significant differences in the activity of a given G protein are indicated with an asterisk (*) ($p < 0.05$). For Gq activity in *Callinectes*, $p < 0.051$ and for Gs activity in *Machrobrachium*, $p < 0.07$.

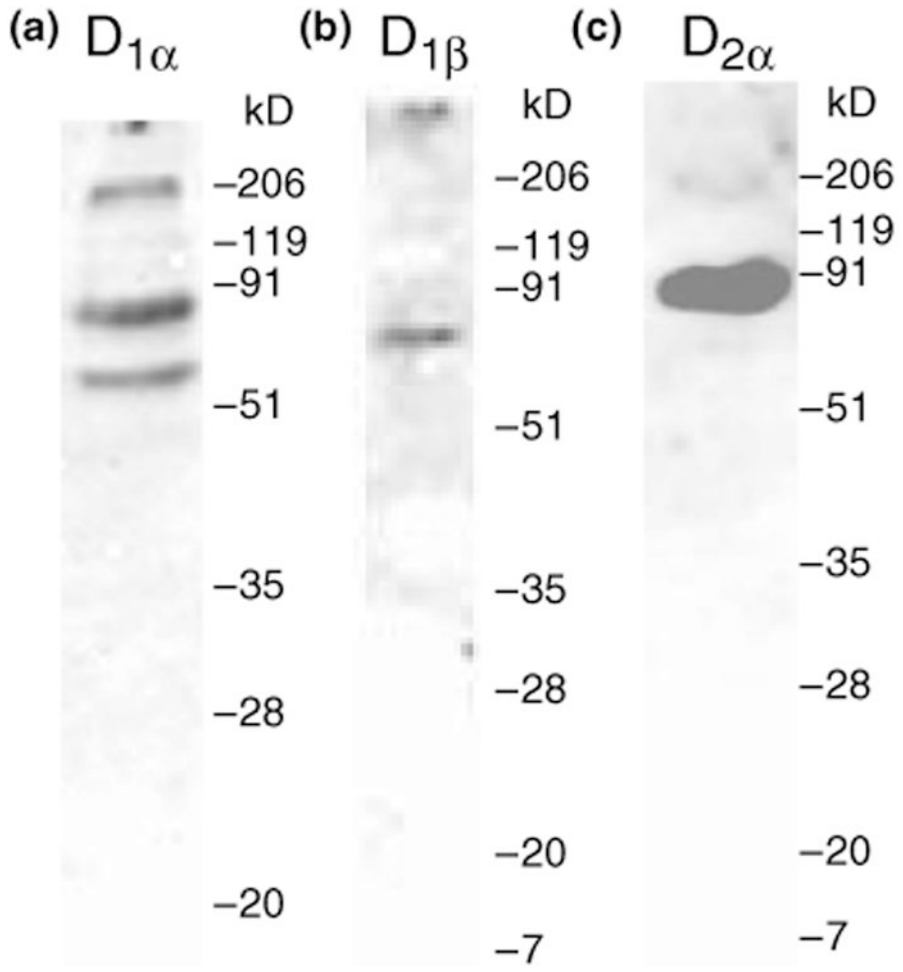

Fig. 4.

Affinity-purified antibodies specifically recognize their respective proteins. Western blots containing protein extracts from the lobster nervous system were probed with anti-$D_{1\alpha Pan}$ (a) or anti-$D_{1\beta Pan}$ (b) or anti-$D_{2\alpha Pan}$ (c) antibodies. For each antibody, nervous systems from multiple lobsters were individually examined ($n \geq 3$). The molecular weight standards for each western blot are indicated. The predicted molecular weights of the receptors are: $D_{1\alpha Pan}$ ~ 76 kDa, $D1_{\beta Pan}$ ~ 48 kDa, $D_{2\alpha Pan}$ ~ 66 kDa.

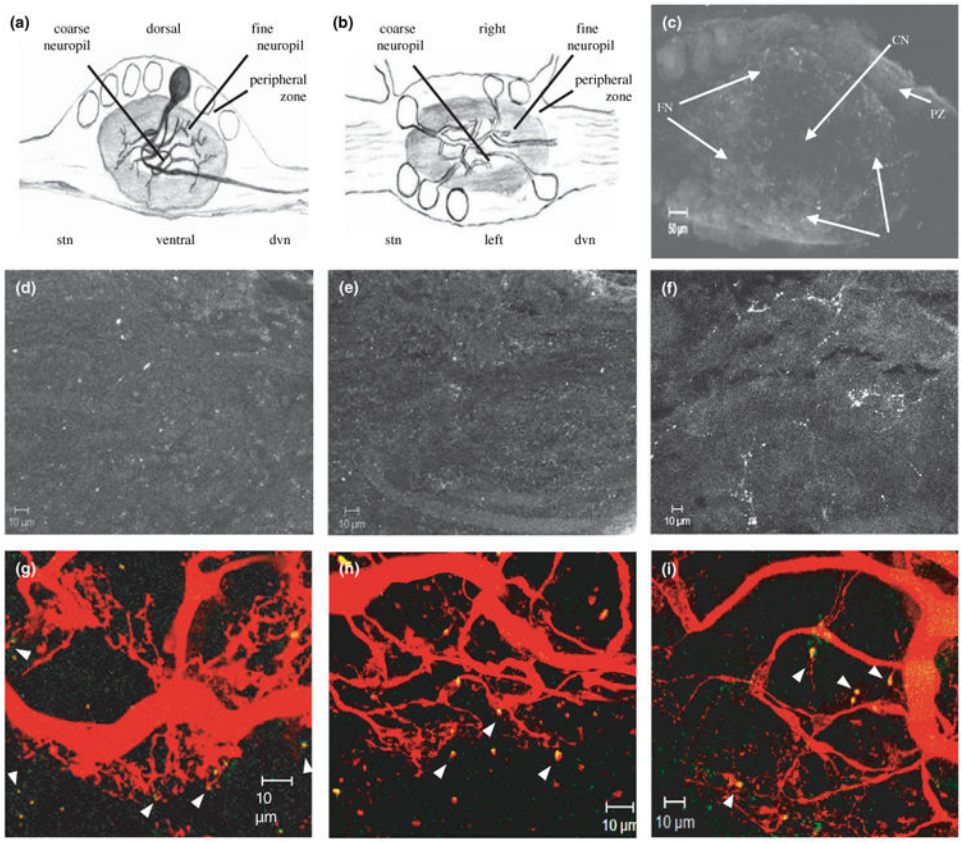

Fig. 5.

DARs are localized to the STG synaptic neuropil. (a) Diagrammatic representation of a midsagittal section through the STG, with a single neuron highlighted. (b) Diagram of a horizontal section through the STG. (c) 21 µm confocal projection from a wholemount STG preparation showing DAR staining in the STG. 3 µm confocal slices from the center of the ganglion were used to construct the low magnification projection shown. Mounting was such that all confocal slices represent horizontal sections through the STG, as shown in B. The arrows point to: fine neuropil (FN), coarse neuropil (CN), and peripheral zone (PZ). Staining appears as white puncta. (d–f), Whole-mount STG preparations stained with anti-$D_{1\alpha Pan}$, $n = 9$ (d) or anti-$D_{1\beta Pan}$, $n = 11$ (e) or anti-$D_{2\alpha Pan}$, $n = 11$ (f) were used to obtain stacks of serial 1 µm confocal optical sections through the synaptic neuropil. The stacks were used to make the 10 µm projections shown. (g–i) Merged confocal projections of STG neurons that were filled with Texas red and stained with anti-$D_{1\alpha Pan}$ (g) or anti-$D_{1\beta Pan}$ (h) or anti-$D_{2\alpha Pan}$ (i). Yellow indicates DAR staining in the filled neurons. Green shows DAR staining in unfilled cells. Projections are 30 µm (g), 26 µm (h), or 48 µm (i). Arrowheads point to putative synaptic terminals containing DARs.

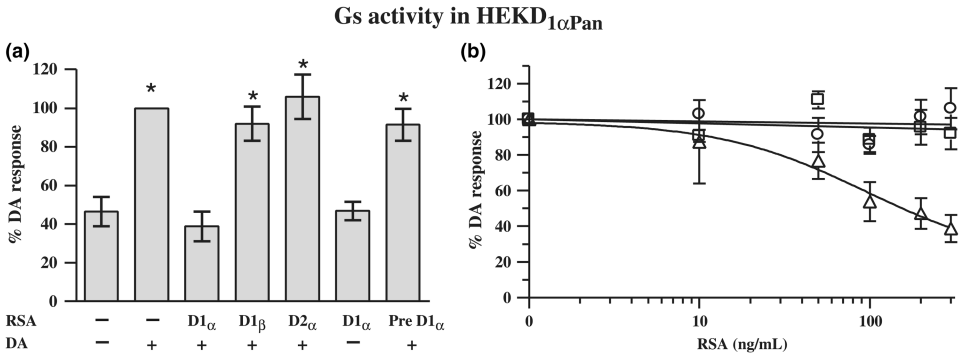

Fig. 6.

Only the $D_{1\alpha}$ RSA can uncouple the $D_{1\alpha Pan}$ receptor from Gs. (a) The left panel shows the effect of each RSA on D_{1Pan} receptor-G protein coupling. Gs activity was measured in HEK $D_{1\alpha Pan}$ membrane preparations in the presence (+) or absence (−) of 10^{-5}mol/L DA and 300 ng/mL of an RSA as indicated under each bar. Data were normalized by G protein activity in the presence of 10^{-5}mol/L DA without RSA, and are plotted as the percent of the response in 10^{-5}mol/L DA without RSA. Pre $D_{1\alpha}$ indicates that the $D_{1\alpha}$ RSA was preabsorbed with its peptide antigen. Asterisks (*) indicate a significant difference from no DA no RSA ($p < 0.05$). Data represent the mean ± SEM, $n \geq 3$. (b) The right panel shows the dose-dependency of RSA uncoupling. Gs activity was measured in HEK $D_{1\alpha Pan}$ membrane preparations in the presence of 10^{-5}mol/L DA and increasing concentrations of an RSA ($D_{1\alpha}$, open triangles; $D_{1\beta}$, open squares, $D_{2\alpha}$ open circles). Data represent the mean ± SEM, $n \geq 3$.

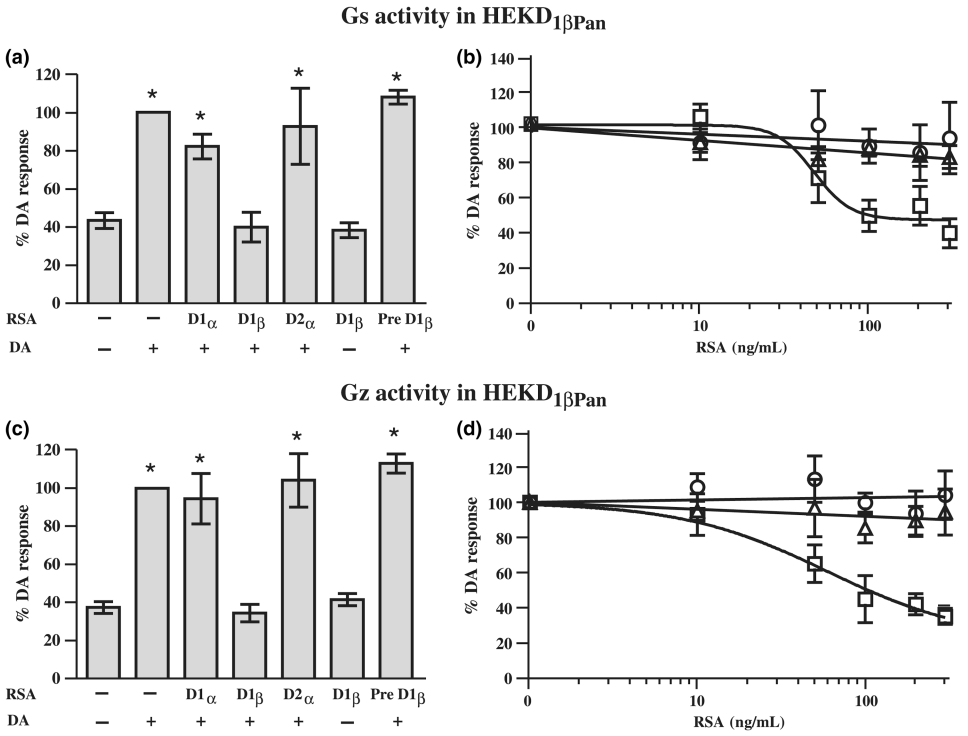

Fig. 7.

Only the $D_{1\beta}$ RSA can produce significant uncoupling of the $D_{1\beta Pan}$ receptor from Gs and Gz. The left panels show the effect of each RSA on $D_{1\beta Pan}$ receptor-G protein coupling. Gs (a) or Gz (c) activities were measured in HEK $D_{1\alpha Pan}$ membrane preparations in the presence (+) or absence (−) of 10^{-5}mol/L DA and 300 ng/mL of an RSA as indicated under each bar. Asterisks (*) indicate a significant difference from no DA no RSA ($p < 0.05$). Data represent the mean ± SEM, $n \geq 3$. The right panels show that RSA uncoupling exhibits a dose-dependency. Gs (b) or Gz (d) activities were measured in HEK $D_{1\beta Pan}$ membrane preparations in the presence of 10^{-5}mol/L DA and increasing concentrations of an RSA ($D_{1\alpha}$, open triangles; $D_{1\beta}$, open squares, $D_{2\alpha}$ open circles). Data represent the mean ± SEM, $n \geq 3$.

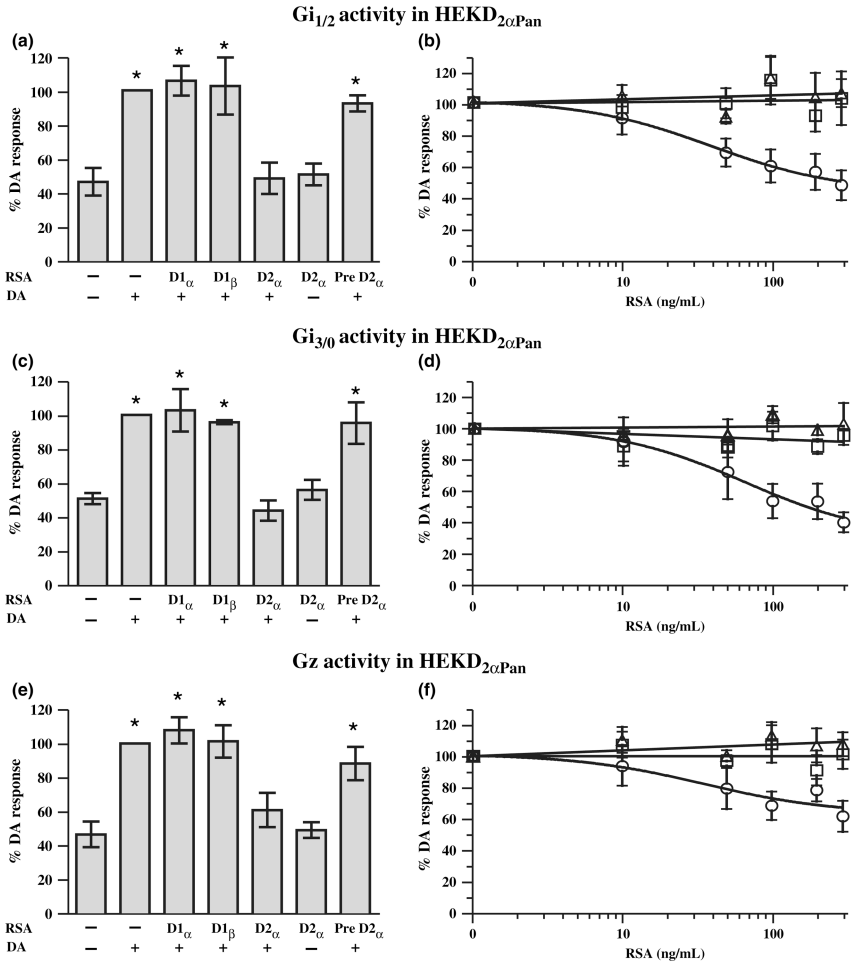

Fig. 8.

Only the $D_{2\alpha}$ RSA can uncouple the $D_{2\alpha Pan}$ receptor from the Gi/o family of G proteins. The left panels show the effect of each RSA on $D_{2\alpha Pan}$ receptor-G protein coupling. Gi_1 and Gi_2 (a) or Gz (c) or Gi_3 and Go (e) were measured in HEK $D_{2\alpha Pan}$ membrane preparations in the presence (+) or absence (−) of 10^{-5}mol/L DA and 300 ng/mL of an RSA as indicated under each bar. Asterisks (*) indicate a significant difference from no DA, no RSA ($p < 0.05$). Data represent the mean ± SEM, $n \geq 3$. The right panels show that RSA uncoupling exhibits a dose-dependency. Gi_1 and Gi_2 (b) or Gz (d) or Gi_3 and Go (f) activities were measured in HEK $D_{2\alpha Pan}$ membrane preparations in the presence of 10^{-5}mol/L DA and increasing concentrations of an RSA ($D_{1\alpha}$, open triangles; $D_{1\beta}$, open squares, $D_{2\alpha}$ open circles). Data represent the mean ± SEM, $n \geq 3$.

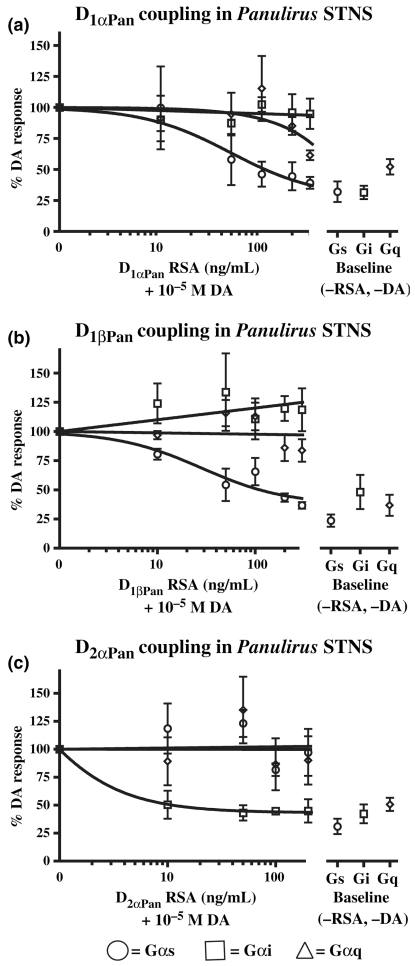

Fig. 9.

DAR-G protein couplings in *Panulirus* STNS membranes. (a) The $D_{1\alpha Pan}$ receptor couples with Gs and Gq, but not Gi, in *Panulirus* STNS membranes. G protein activities (Gs, circle; Gi, square; Gq, diamond) in *Panulirus* STNS membrane preparations were measured either in the presence of 10^{-5}mol/L DA and increasing concentrations of the $D_{1\alpha}$ RSA, or in the absence of DA and the RSA (baseline conditions). Two STNS were used per experiment, and the experiment was repeated four times. Thus, each data point in panel A represents 8 lobsters. Data are represented as the mean ± SEM. (b) The $D_{1\beta Pan}$ receptor couples with Gs, but not Gq or Gi, in *Panulirus* STNS membranes. G protein activities (Gs, circle; Gi, square; Gq, diamond) in *Panulirus* STNS membrane preparations were measured either in the presence of 10^{-5}mol/L DA and increasing concentrations of the $D_{1\beta}$ RSA or in the absence of DA and the RSA (baseline conditions). Two STNS were used per experiment, and the experiment was repeated three times. Thus, each data point in panel b represents 6 lobsters. Data are represented as the mean ± SEM. (c) The $D_{2\alpha Pan}$ receptor couples with Gi, but not Gs or Gq, in *Panulirus* STNS membrane preparations. G protein activities (Gs, circle; Gi, square; Gq, diamond) in *Panulirus* STNS membrane preparations were measured either in the presence of 10^{-5}mol/L DA and increasing concentrations of the $D_{2\alpha}$ RSA or in the absence of DA and the RSA (baseline conditions). Two STNS were used per experiment,

and the experiment was repeated three times. Thus each data point in panel c represents six lobsters. Data are represented as the mean ± SEM. In all, 20 lobsters were used in these experiments (8, panel a + 6, panel b + 6, panel c).